ACEM Journal

Copy of e-mail Notification

ACEM Published by ASTM

Dear Author,

YOUR PAGE PROOF IS AVAILABLE IN PDF FORMAT; please refer to this URL address
http://115.111.50.156/jw/AuthorProofLogin.aspx?pwd=e4c33133e1e9&CA=AT

Login: your e-mail address
Password: e4c33133e1e9

The site contains 1 file. You will need to have Adobe Acrobat Reader software to read these files. This is free software and is available for user downloading at http://www.adobe.com/products/acrobat/readstep.html.

This file contains:
Adobe Acrobat Users - NOTES tool sheet
A copy of your page proofs for your article

Please read the page proofs carefully and:

1) indicate changes or corrections using e-annotation;
2) answer all queries;
3) proofread any tables and equations carefully;
4) check that any special characters have translated correctly.

Special Notes:

Your edits must be returned (uploaded or emailed) within 48 hours of receiving page proofs to review. Please notify Denise Stanley (denise.stanley@cenveo.com) immediately if you anticipate a delay in returning your edits.

Your Login and Password are valid for a limited time. Your prompt attention to and return of page proofs will help expedite publication of your work. Thank you for your cooperation.

If you have any questions regarding your article, please contact me. PLEASE ALWAYS INCLUDE YOUR ARTICLE NO. (ACEM20120043.R1) WITH ALL CORRESPONDENCE.

Posting Author Papers on Website Policy—Author’s Rights as Stipulated in the Accepted Electronic Agreement during Paper Submission:

“The right to post the pre-print version of the Work on your website or your employer’s website with reference to the publication by ASTM as the copyright holder. This preprint will be sent to you by the copyeditor. This version does not include the final edits. Such preprints may be posted as electronic files on the Author's own website for personal or professional use, or on the Author's internal university or corporate networks/intranet, or secure external website at the Author's institution, but not for commercial sale or for any systematic external distribution by a third party (eg: a listserver or database connected to a public access server). Prior to publication, the Author must include the following notice on the preprint: "This is a preprint of an article accepted for publication in (Journal Title Copyright @ (year) (copyright ASTM International, West Conshohocken, PA)10.1520/ACEM20120043". After publication of the Work by ASTM International, the preprint notice should be amended to read as follows: "This is a preprint of an article published in (include the complete citation information for the final version of the Work as published in the print edition of the Journal)" and should provide an electronic link to the Journal's WWW site, located at the following ASTM URL: http://www.astm.org/10.1520/ACEM20120043. The author agrees not to update the preprint or replace it with the published version of the Work."

Sincerely,
Denise Stanley, Journal Production Manager
E-mail: Denise.Stanley@cenveo.com

Reprints Order Form

For reprints of articles and/or papers from ASTM Journals, Selected Technical Papers (STPs), book chapters and *Standardization News.*

Note: Authors receive a 25% discount

Ship To:
Name: ______________________________

Organization: ______________________________

Address: ______________________________

City: ______________________ State: ____________ Zip: ________

Country: ______________________________

Bill To:
Name: ______________________________

Organization: ______________________________

Address: ______________________________

City: ______________________ State: ____________ Zip: ________

Country: ______________________________

Date:	Phone:	email:	Fax:

Paper Title: ______________________________

Publication: ______________________________
(Title, month, and volume number; STP number; or stock number)

Page length of article: ____________ **Number of copies:** (25 copies minimum) ____________

Cover: (check one)

❑ Reprinted article, no cover

❑ Reprinted article and cover with typeset title of article and author's name

Questions about your order?
Call Customer Relations at 610/832-9585, weekdays 8:30am–4:30pm ET

Complete Quote request and Return to:
1. service@astm.org
2. **Fax:** 610/832-9555
3. **Mail to:**
   Customer Relations
   ASTM International Customer Service
   100 Barr Harbor Drive
   West Conshohocken, PA 19428-2959

ASTM INTERNATIONAL
Standards Worldwide

Reprints Price Scale*

Color Reprints

Pages \ Copies	100	200	500	1000	2000
2	$1,102	$1,323	$1,543	$1,764	$1,984
3-4	$2,116	$2,221	$2,326	$2,425	$2,824
5-8	$2,168	$2,278	$2,394	$2,499	$3,024
9-12	$3,307	$3,470	$3,638	$3,801	$4,126

Black & White Reprints

Pages \ Copies	25	50	100	200	300	500	100 0	2000
1-4	$136	$152	$168	$184	$199	$226	$310	$472
5-8	$195	$226	$257	$278	$299	$352	$499	$709
9-12	$225	$257	$289	$336	$357	$425	$577	$787
13-16	$263	$294	$325	$394	$430	$520	$751	$1,118
17-20	$278	$336	$394	$472	$514	$635	$887	$1,307
21-24	$301	$373	$446	$535	$583	$724	$1,003	$1,475
25-28	$331	$404	$478	$583	$646	$808	$1,165	$1,795
29-32	$383	$441	$499	$651	$724	$913	$1,323	$2,058
Cover (optional)	$100	$115	$136	$157	$178	$220	$373	$598

* Prices are subject to change without notice.

ASTM International Customer Relations department will finalize your reprint quote including freight charges. ASTM International will contact you with the quote price.

AUTHOR QUERY FORM

ASTM INTERNATIONAL Standards Worldwide	**Journal:** **Adv. Civ. Eng. Mater.** **Article Number:** **ACEM20120043**	**Please provide your responses and any corrections by annotating this PDF and uploading it to ASTM's eProof website as detailed in the Welcome email.**

Dear Author,

Below are the queries associated with your article; please answer all of these queries before sending the proof back to Cenveo. Author please indicate the correct color processing option from the list below:

1. Author, please confirm Figure number(s) that should appear as color in print. Please know that any associated mandatory fees will apply for figures printed in color.
2. Author, please confirm Figure number(s) that should appear as color online only, there will be no fees applied.
3. Author, your paper currently does not include any color figures for online or print. If color is needed please indicate which figures it should be applied to and whether it is color in print or online.

Location in article	**Query / Remark: click on the Q link to navigate to the appropriate spot in the proof. There, insert your comments as a PDF annotation.**
AQ1	Please provide the name and location of the sponsoring organization in Ref. 10.

Thank you for your assistance.

Advances in Civil Engineering Materials, Vol. 2, No. 1
Paper ID ACEM20120043
www.astm.org

J. Giraldo[1] *and M. T. Rayhani*[2]

Influence of Fiber-reinforced Polymers on Pile–Soil Interface Strength in Clays

REFERENCE: Giraldo, J. and Rayhani, M. T., "Influence of Fiber-reinforced Polymers on Pile–Soil Interface Strength in Clays," *Advances in Civil Engineering Materials*, Vol. 2, No. 1, 2013, pp. 1–17, doi:10.1520/ACEM20120043. ISSN 2165-3984.

ABSTRACT: A series of direct shear tests were carried out in order to characterize the pile–soil interface strength for various pile materials including steel, concrete, and grout and to investigate the influence of fiber-reinforced polymer (FRP) materials on the pile–soil interface strength in soft clay. The study investigated both pile–soil interface friction and interface adhesion by simulating drained and undrained conditions. The results among the traditional pile materials indicated the superior performance of grout and concrete relative to steel. FRP interfaces were shown to perform at a level the same as or higher than that of traditional steel piling under both drained and undrained conditions in clays. The FRP–clay interface friction angles were 5 % to 19 % greater than those in traditional steel–clay interfaces and 12 % to 23 % smaller than that of concrete. In addition, FRP interface adhesion was observed at between 86 % and 135 % of the interface adhesion of steel and between 65 % and 75 % of the interface adhesion of concrete.

KEYWORDS: pile, interface, direct shear, shear strength, capacity, FRP, clay, roughness, composite

Introduction

The shear resistance between soils and an interface surface is of significant interest for the design and performance of many geotechnical systems such as friction piles, bored piles, soil nails, anchor rods, retaining walls, and geomembranes, among others. This interface shear resistance depends on the soil type, grain size distribution, interface material, surface roughness, normal stresses at the interface, and rate of shear displacement [1]. Significant work has been completed on the interface characterization of typical pile materials with sandy soils relative to work performed on clayey soils and, in particular, in sensitive marine clays [2].

In recent decades, new composite materials have been rising in popularity as construction materials, particularly in structural rehabilitation and the construction of new buildings. These composite materials, known as fiber-reinforced polymers (FRPs), present significant benefits when used in conjunction with steel and concrete construction by improving the strength and service life of the structure. In recent years, initiatives have been made by different researchers, government agencies, and FRP manufacturers to use FRP materials in piling and geotechnical applications. In turn, this effort has produced interest regarding the performance of FRP piles in different soil conditions. However, the use of FRPs in the piling industry is largely limited to marine fender piles, load-bearing piles for light structures, and pilot test projects [3]. In particular, previous research has

Manuscript received October 17, 2012; accepted for publication August 26, 2013; published online xx xx xxxx.

[1]Research Assistant, Dept. of Civil and Environmental Engineering, Carleton Univ., Ottawa, ON, Canada K1S 5B6 (Corresponding author), e-mail: juan.giraldovelez@alumni.carleton.ca

[2]Assistant Professor, Dept. of Civil and Environmental Engineering, Carleton Univ., Ottawa, ON, Canada K1S 5B6.

focused on improving areas where traditional piling materials face significant vulnerabilities, such as in harsh marine environments, where the degradation of pile materials can lead to a decrease in structural and geotechnical pile capacity [4], thus reducing the structure's service life. Studies completed on the performance of FRP piles are almost exclusively limited to the behavior of FRP interfaces in sandy soils; seldomly do studies explore the interaction of clayey soils with these composite materials.

Shear strength studies carried out by Pando et al. [5] on FRP–sand interfaces showed that the angle of friction increases as the relative surface roughness height increases. In addition, surface hardness and particle angularity interact; a greater interface friction angle was observed when angular sands sheared against a relatively softer FRP material, because the sand particles penetrated into the surface. Conversely, a smaller friction angle was observed when relatively rounder sand particles were sheared against a harder FRP surface, because the particles tended to slide. Pre-stressed concrete pile surfaces presented the greatest interface friction angles because of their rougher surface topology, which leads to complex particle-interlocking mechanisms. A similar study conducted by Frost and Han [4] showed a linear increase of the friction angle with the relative surface roughness, while little influence on the interface shear parameters was found because of the rate of shearing or sample thickness. In addition, the results indicated similar interface friction and surface roughness parameters in the FRP specimens and in steel, which illustrates the viability of using FRP materials as piling materials in granular soils. Studies carried out by Chu and Yin [6] on the strength properties of grout–soil interfaces demonstrated that the interface friction angle was influenced by the moisture content of the soil sample and the grout surface shape. Research on grout–soil interface strength is limited, and shear strength parameters in different soil types are generally limited to results derived from pile-load tests of soil nails or micropiles.

Interface shear strength characterization in clayey soils has not been studied as extensively as in sands; however, the importance of shear strength characterization in clays was highlighted by Skempton [7] in regard to slope stability analysis by measuring the clay residual strength in a shear box apparatus. Lupini et al. [8] carried out a comprehensive study on the drained residual strength of cohesive soils using a ring shear apparatus and identified three principal shear failure modes in cohesive soils: turbulent, transitional, and sliding. The shearing behavior was determined to be dependent on the shape and type of soil particles and on the ratio between rotund and platy particles. Stark and Eid [9] carried out similar work using a ring shear apparatus on a number of different cohesive soils and concluded that the drained residual shear strength is dependent on the mineral type and the clay fraction of the soil. Studies carried out by Lemos and Vaughan [1] on clay against smooth glass and steel interfaces linked the failure modes observed in pure soil shearing to the clay content of the soil and the surface roughness. Soils with a high clay fraction that undergo sliding shear failure tend to reach soil–soil shear strength and are independent of surface roughness, whereas soils with lower clay contents are dependent on the surface roughness, as larger soil particles interact with the material interface. Various studies have been carried out to test different interfaces used in the construction and piling industry against various types of clays [6,10–13]. Results from these tests provide robust data regarding the shear interface behavior for various conditions and materials; however, few, if any, interface shear testing programs have characterized the shear interface strength between clayey soils and FRP materials to the extent that it has been studied in sands.

The goal of this paper is to investigate the interface shear strength properties of various piling materials and compare their performance with the interface shear resistance achieved by FRP surfaces. Interface materials tested in this research include steel, concrete, grout, and two types of FRP surfaces. This work focuses on using a direct shear box apparatus in order to obtain interface shear strength parameters, expressed as the effective interface friction angle δ and the apparent interface adhesion c_a, by testing each interface specimen under drained and undrained conditions. The results will help in determining, from a geotechnical point of view, the suitability of FRP materials in piling and other applications where the soil–structure frictional interface is of importance. In addition, results from this work will provide some insight into the mechanisms of soil–FRP interaction, such as the influence of surface roughness, the epoxy matrix, and FRP fiber orientation, allowing one to determine the optimal parameters for the best frictional interface performance.

Material Properties

Soil Properties

The soil used in this study was a marine clay known as Leda clay or Champlain Sea clay, which covers the Ottawa Valley and southern Quebec. The clay material formed near the end of the most recent glaciation period in the pre-historic Champlain Sea, where fine sediments and rock flour generated from glacial abrasion of the Canadian Shield settled to form thick deposits of Leda clay along the St. Lawrence drainage basin.

Intact clay samples were obtained from a known clay-rich site at a local landfill in Ottawa, ON, Canada, from a depth of 2 to 3 m. Atterberg limit tests were carried out in accordance with ASTM D4318-10 [14] and showed a plastic index of 22 %. In order to establish the particle size distribution, a hydrometer test was carried out in accordance with ASTM D422-63 [15], and the results showed a 40 % clay fraction and an activity of 0.55 (Fig. 1). The soil is classified as CH according to the Unified Soil Classification System [16]. The undrained shear strength of the soil was determined by performing a vane shear test in accordance with the field vane shear test procedure outlined in ASTM D2573-08 [17]. The undrained soil shear strength was determined to be $S_u = 50$ kPa. The coefficient of one-dimensional consolidation was measured according to ASTM D2435/2435M-11 [18] and had a value of 1.4×10^{-4} cm^2/s. A direct shear box testing program according to ASTM D3080/D3080M-11 [19] was performed on intact clay specimens in order to determine their drained and undrained shear strength parameters. The shearing rates used were 0.05 mm/min for drained conditions and 2.5 mm/min for undrained conditions. The index properties of the Leda clay used in this study are summarized in Table 1. The soil properties measured for the Leda clay specimens in this study correlate fairly well with previously published work on Leda clay–interface interactions [13,20].

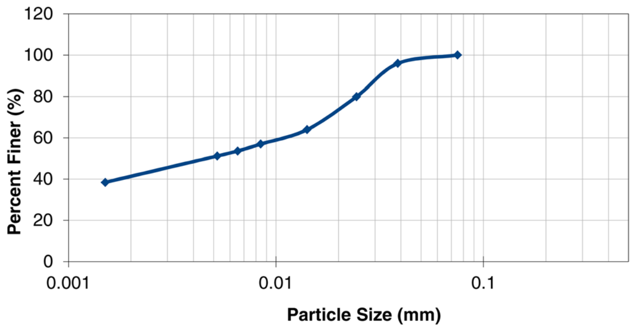

FIG. 1—*Leda clay grain size distribution.*

J_ID: ACEM DOI: 10.1520/ACEM20120043 Date: 3-September-13 Stage: Page: 4 Total Pages: 18
PROOF COPY [ACEM20120043]

TABLE 1—*Leda clay soil properties.*

ρ, Mg/m^3	w, %	LL, %	PI, %	w_{opt}, %	$\rho_{d(max)}$, Mg/m^3	c_v, cm^2/s	s_u, kPa	ϕ, deg	c_u, kPa
1.53	49	51	23	14	1.85	1.00×10^{-4}	50	23.3	42.2

Notes: ρ, density; w, moisture content; w_{opt}, optimum moisture content; $\rho_{d(max)}$, maximum dry density; c_v, coefficient of consolidation; s_u, undrained shear strength; ϕ, internal friction angle; c_u, apparent cohesion.

Pile Interfaces

The interface between the soil and the pile material plays a critical role in determining the frictional capacity along the shaft of the pile. In this study, several pile material interfaces were studied in order to establish the shear strength properties in Leda clay. The interface materials tested were steel, concrete, cement grout, carbon fiber-reinforced polymer (CFRP), and glass fiber-reinforced polymer (GFRP).

Interface Roughness

Surface roughness has been shown to influence the interface shear strength of non-cohesive soils [21–23] and cohesive soils [1]. Various definitions of surface roughness have been proposed in the study of interface shear in sands. Macro-roughness describes the undulations along the surface, which cause extra internal work if the shearing follows this path [24]. Microroughness is relevant at the scale of the particle size of the soil being sheared against the surface. For this study, macro-roughness is relevant for the FRP surface samples, as the glass and carbon fibers form a distinctive surface waviness which can influence the clay shearing interface. Surface roughness was measured by using a FARO arm measuring device to scan each interface surface across a linear path and recording the vertical tip deviations. Various surface roughness description techniques have been proposed. Kishida and Uesegui [25] used a normalized roughness value R_n, based on the median particle grain size distribution $D_{50.}$ This normalized surface roughness takes into account both the surface roughness of the material and how it interacts with the soil based on its particle size. A more simplified approach is taken in this study by calculating interface roughness as the average of the displacements measured at each data point, known as a center line average or total roughness R_t, and by calculating the root mean square of the same dataset to determine the average roughness R_a, illustrated as follows:

$$R_t = \frac{h_1 + h_2 + \cdots + H_n}{n}, \quad R_a = \sqrt{\frac{h_1^2 + h_2^2 + \cdots + H_n^2}{n}} \tag{1}$$

Steel Interface

A common pile material used in industry is structural steel. Typical pile shapes include circular steel pipes and H steel sections. The benefits of steel piles include high load capacity, drivability, and high structural capacity; their disadvantages include the vulnerability of steel to corrosion in harsh environments and high steel costs. Steel plates were prepared in order to simulate the wall surface of a typical steel pile. The specimens were 90 mm by 90 mm square steel plates with a thickness of 0.5 in. (12.5 mm) machined to couple with the upper half of the direct shear box apparatus (Fig. 2). The total surface roughness value R_t was 9.7 μm, and the average roughness R_a was 11.3 μm (Table 2).

ID: veeraragavanb Time: 21:12 I Path: S:/3B2/ACEM/Vol00201/130035/APPFile/AT-ACEM130035

J_ID: ACEM DOI: 10.1520/ACEM20120043 Date: 3-September-13 Stage: Page: 5 Total Pages: 18

PROOF COPY [ACEM20120043]

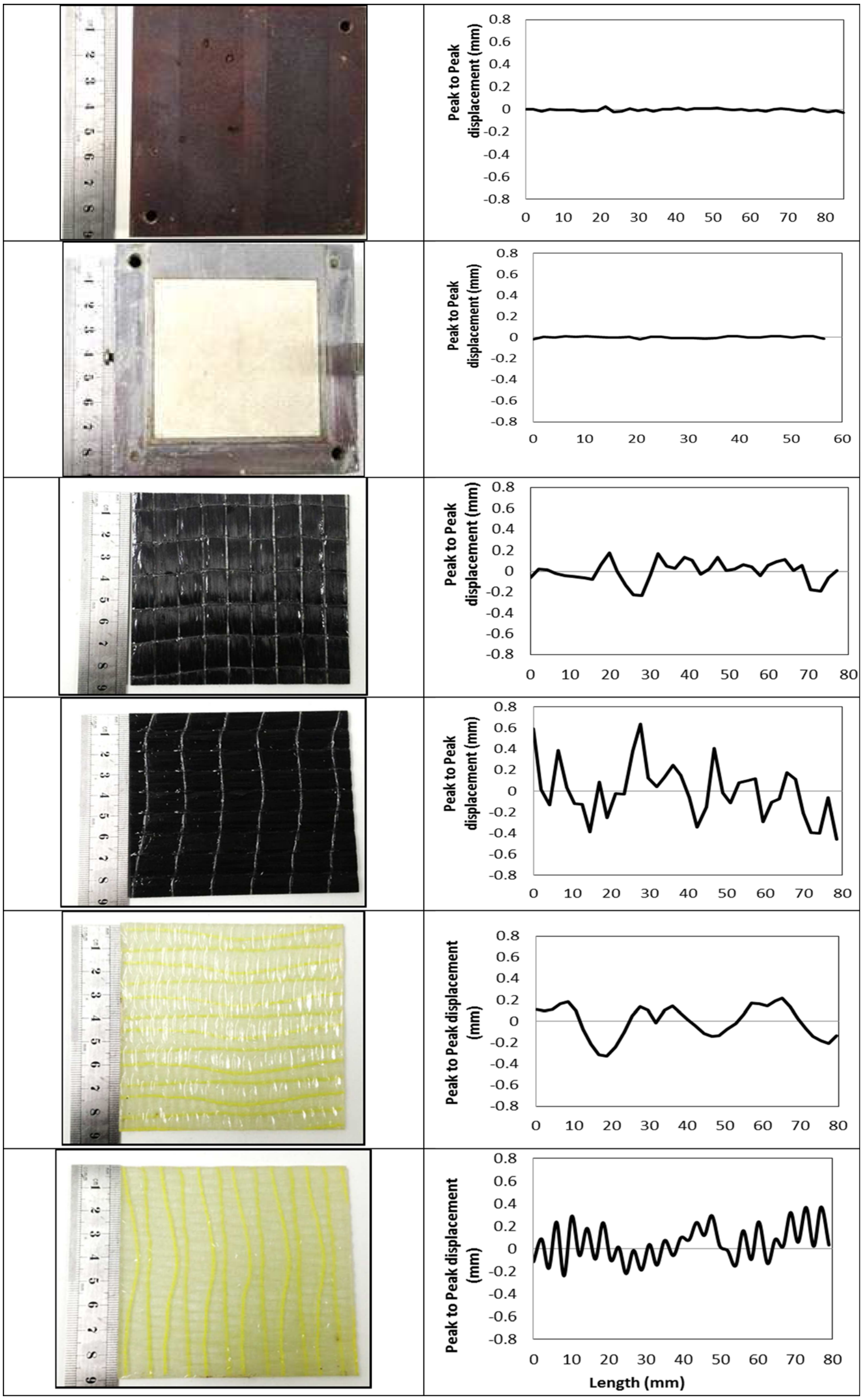

FIG. 2—*Surface interface and profile for steel, concrete, CFRP at 90°, CFRP at 0°, GFRP at 90°, and GFRP at 0°.*

ID: **veeraragavanb** Time: 21:12 I Path: S:/3B2/ACEM/Vol00201/130035/APPFile/AT-ACEM130035

TABLE 2—*Pile interface roughness.*

Interface	R_t, μm	R_a, μm
Steel	9.7	11.3
Concrete	7.5	9.1
Carbon at 90°	200	250
Carbon at 0°	76	99
Glass at 90°	130	149
Glass at 0°	140	173

Concrete Interface

A concrete sample was prepared by using a pre-mixed cement–fine sand grout with a 1:3 ratio of sand to cement and a 35 % water content by weight. The sample was cast in the lower portion of a shear box device, sealed with a flat Plexiglas surface to ensure a smooth and level surface finish, and allowed to cure for 14 days prior to initial testing (Fig. 2). The total surface roughness value R_t was 7.1 μm, and the average roughness R_a was 9.1 μm.

Grout Interface

The grout interface testing simulated the behavior of typical cast-in-place piles such as micropiles drilled in soil. In order to appropriately simulate the interface, neat cement grout was prepared with a ratio of 60 % cement to 40 % water by weight and cast in the bottom half of a shear box device, with an intact clay sample placed in the upper half. The shear box was reassembled, sealed with silicone caulking, and allowed to cure for 14 days to allow the grout–soil bond to develop prior to interface testing. This approach was intended to simulate the behavior of gravity-poured cast-in-place piles in the field. Because of the nature of the grout–ground bonding interface, the surface roughness was not measured.

Carbon and Glass Fiber-reinforced Polymer Interface

Two types of FRP materials were used in this study: CFRP and GFRP. These FRP systems consist of a two-part mechanism: a carbon or glass woven fabric, and a corresponding epoxy resin acting as the matrix medium for the fiber.

The clay–FRP interface was prepared by manufacturing a 10 in. by 10 in. double-layered flat sheet of each material that was then water-jet cut into coupons sized to match the bottom half of a shear box device. The surface texture of each material had a distinctive shape with a surface waviness controlled by how the material fabric was woven and the finish resulting from the application of the epoxy. Both specimens were manufactured per the manufacturer's instructions using epoxy-saturated foam paint rollers, and the achieved surface textures were left to cure. The surface profiles and topology were significantly different based on the fiber orientation (Fig. 2).

Experimental Procedures

The interface characterization program was carried out using a direct shear test apparatus according to ASTM D3080/D3080M-11 [19] and ASTM D5321-12 [26]. The direct shear test apparatus consists of a displacement controlled testing apparatus used to apply a fixed displacement rate to the shear box device through a series of gearing mechanisms. The shear box has inside specimen dimensions of 60 mm by 60 mm, outside dimensions of 90 mm by 90 mm, and a specimen height of 25.4 mm. The confining pressure is applied by a steel bearing arm using weights to apply vertical

J_ID: ACEM DOI: 10.1520/ACEM20120043 Date: 3-September-13 Stage: Page: 7 Total Pages: 18
PROOF COPY [ACEM20120043]

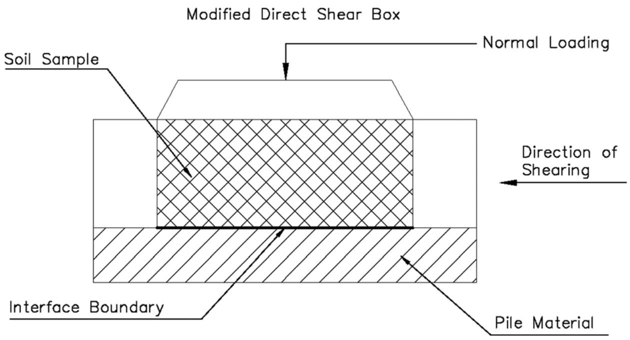

FIG. 3—*Schematic of the modified shear box.*

stresses to the specimen. The shearing stresses are measured through a digital load cell connected horizontally to the top section of the shear box. Horizontal and vertical displacements are measured through a linear variable differential transducer connected to a digital logging station using LabView software. We modified the shear box device slightly by replacing the lower half of the standard direct shear box with the interface material for interface tests. A schematic of the modified apparatus is illustrated in Fig. 3.

Loading Rates

Two loading rates were used for each test in order to simulate both drained and undrained conditions. Drained conditions were achieved by using a shearing rate of 0.05 mm/min or 5 % strain per hour in order to allow pore water pressure dissipation and measurement of the effective interface friction angle ϕ'. Although the drained rate ideally achieves complete pore water dissipation, because of the very low hydraulic conductivity of the clay, it is unrealistic to expect true drained conditions, and some excess pore water pressure generation will be developed while shearing. Undrained conditions were achieved by using a shearing rate of 2.5 mm/min in order to measure the interface adhesion component c_a. Additionally, a nonporous support located at the upper portion of the sample where the loading plate was applied was used to reduce drainage and ensure undrained conditions. The shearing rates were kept consistent throughout the testing for all interfaces in order to objectively compare the shear strength parameters independently of the rate effects, which can have an influence on the residual shear strength parameters of soil-on-soil tests [8] and soil-on-interface tests [1].

Soil–Interface Specimen Preparation

Five different soil–interface materials were tested: steel, concrete, grout, and two types of FRPs. For the steel–soil interface, a square plate of mild steel was placed in the lower half of the shear box, and an undisturbed specimen of Leda clay was carefully cut to match the upper-half opening of the box and fitted to ensure complete steel–clay contact at the interface. The concrete interface was made by filling the lower half of the shear box with a concrete mix and allowing it to cure against a smooth Plexiglas surface in order to create a smooth shearing surface similar to that of pre-stressed concrete piles. The box was reassembled and a clay specimen was fitted, ensuring complete interface contact.

The grout interface was created by pouring a fresh neat cement grout mix in the bottom half of the shear box and leveling it with a metal edge; subsequently, the top half of the shear box was carefully fitted with a clay sample. The device was carefully assembled, ensuring interface contact of the two materials at the midplane of the box, and then allowed to cure for 14 days under saturated conditions. This method ensures grout–ground bonding conditions that resemble those of soil nails or micropile gravity grouting in the field.

Finally, the FRP surfaces were created by manufacturing coupons of each material to carefully fit on top of the lower half of the shear box. A metal stopper was attached to the underside of the FRP coupon in order to lock it against the inside edge of the shear box and prevent any slippage of the interface. A clay sample was then carefully fitted on the reassembled shear box in order to ensure complete clay–FRP contact.

Testing Procedure

Interface testing was carried out in accordance with ASTM D3080/D3080M-11 [19]. The modified shear box device was placed within a metal container that was laid upon a set of linear ball bearings allowing unrestricted horizontal displacement. The containing metal box was filled with water to ensure saturated conditions and to prevent cracking of the clay along the interface. The normal loading was applied through a steel bearing arm connected to the top section of the shear box. Three different confining pressures of 50, 100, and 150 kPa were applied to simulate typical lateral earth pressures along the pile shaft at a moderate driving depth. The confining pressure was applied until the vertical settlement normalized to a constant value. Horizontal shearing was then initiated on the sample.

The shearing rates applied were achieved through the use of a precise screw-type actuator calibrated to 0.05 mm/min and 2.5 mm/min in order to achieve drained and undrained conditions, respectively. The shearing was carried out up to a strain of 8 % to 12 % or until residual shear strength conditions had stabilized. Sample strain was calculated based on the linear dimension of the shear box along the direction of shearing. Following failure of the specimen, the assembly was dismantled and a visual inspection of the shearing surface was carried out in order to identify the possible failure mechanism acting along the interface.

Results

Pile Interface Shear Strength

Direct shear tests were carried out on three typically used pile materials—steel, concrete, and grout—against clay under three different confining pressures of 50, 100, and 150 kPa. In order to characterize the shear strength parameters of the interface, two rates of shear displacement were used to determine the interface friction angle ϕ' and the interface adhesion value c_a. Shear stress versus horizontal displacement curves illustrate the failure mechanism at the interface and the influence of the shearing rate.

Drained Conditions

Figure 4(*a*) illustrates the shear stress-strain curve for steel–, concrete–, grout–, and clay–clay interfaces for a 100-kPa confining pressure. In all four cases friction was mobilized at very low displacements, in the range of 0.5 % to 1 % horizontal strain. The grout–, steel–, and clay–clay interfaces reached a peak shear stress value and maintained a constant residual strength at or nearing the peak value measured. In contrast, the concrete interface specimen experienced strain hardening behavior and reached a maximum value at a strain level of 7 % before stabilizing to a constant residual shear strength. The steel interface shearing strength was lower than that of clay, whereas

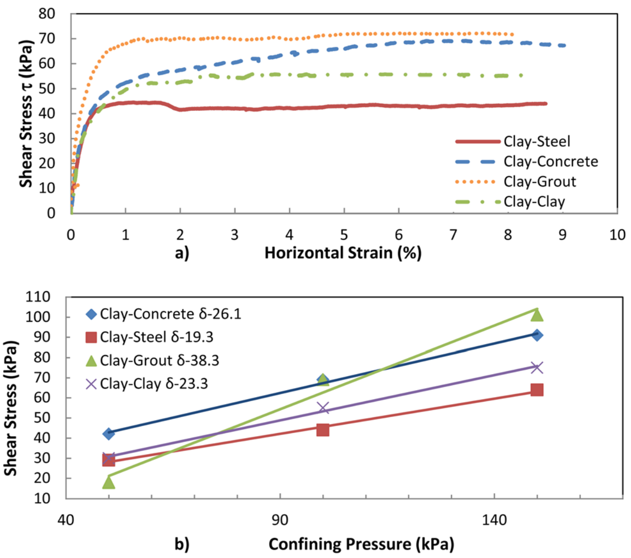

FIG. 4—*(a) Shear stress-strain at 100 kPa. (b) Failure envelopes under drained conditions.*

both grout and concrete interfaces presented higher strength values [Fig. 4(*a*)]. According to Lupini et al. [8] and Lemos and Vaughan [1], shear strength in clays and clay interfaces can be related to the type of failure at the interface, dictated by the ratio of rotund to platy particles in the soil, which can be related by the clay fraction. At a high ratio of rotund particles, these particles tend to rotate, neglecting the effect of the orientation of the platy particles; this is known as turbulent shearing. At larger clay fractions, sliding of the platy particles tends to occur because of the well-defined particle orientation, leading to lower shear strength; this failure mode is known as sliding shear. A third, intermediate state known as transitional shear occurs in between the rotational and sliding shear behaviors. Typically, interface friction angles of more than 25° can be attributed to a turbulent shear mode [2]. The failure envelopes [Fig. 4(*b*)] follow a Mohr–Coulomb failure mechanism illustrating a greater friction angle for grout and concrete, followed by that of steel. Table 3 summarizes the results in terms of the ratio between the interface frictional angle and the clay internal frictional angle δ/Φ'.

Undrained Conditions

Tests carried out under undrained conditions were used to determine the cohesion of the soil and the apparent adhesion between the different interface surfaces and clay. Figure 5(*a*) illustrates the shear stress-strain curve for the different interfaces at a constant normal stress of 100 kPa. As shown, the frictional strength was mobilized at very low horizontal strains in the range of 0.5 % to 1 %, reaching peak shear strength and quickly collapsing to a residual strength state. The steel and concrete interfaces stabilized at a horizontal strain of 2 %, whereas the grout interface experienced strain softening until a deformation of 7 % strain before reaching residual strength conditions. The clay specimen experienced strain hardening behavior until reaching peak strength at 3 % of horizontal strain and a strain softening region until stabilizing at 8 % strain to reach a residual strength state. Figure 5(*b*) illustrates the failure envelopes for the different interfaces exhibiting Mohr–Coulomb behavior. Table 3 summarizes the results in terms of the ratio of the interface adhesion to the soil's apparent cohesion c_a/c. The results for concrete interfaces indicate good agreement with

TABLE 3—*Comparison of shear strength properties of typical pile materials and FRPs.*

Interface Friction Angle

Interface	Φ, deg	δ, deg	δ/Φ, deg	Percentage of Steel Capacity, %	Percentage of Concrete Capacity, %
Grout	23.3	38.3	1.64	—	—
Concrete	23.3	26.1	1.12	—	—
Steel	23.3	19.3	0.83	—	—
C90	23.3	23.0	0.97	119	88
G90	23.3	20.2	0.86	104	77
G0	23.3	22.1	0.92	113	84
C0	23.3	20.4	0.87	105	78

Interface Apparent Adhesion

Interface	c, kPa	c_a, kPa	c_a/c, kPa	Percentage of Steel Capacity, %	Percentage of Concrete Capacity, %
Grout	42.2	43	1.02	—	—
Concrete	42.2	26.3	0.62	—	—
Steel	42.2	14.3	0.34	—	—
C90	42.3	17.3	0.40	120	65
C0	42.3	12.3	0.29	86	46
G90	42.3	19.9	0.45	135	75
G0	42.3	18.3	0.43	127	70

the accepted ratio of 0.7 in terms of the soil cohesion; however, the steel interface presented an adhesion/cohesion ratio of 0.33, which can be attributed to the relatively smoother surface of the steel in comparison with the concrete and the possible absorption of pore water by the concrete. Similar to the drained results, the grout–soil case presents a higher interface adhesion than pure soil, which can be attributed to the bonding and interaction between the soil and grout.

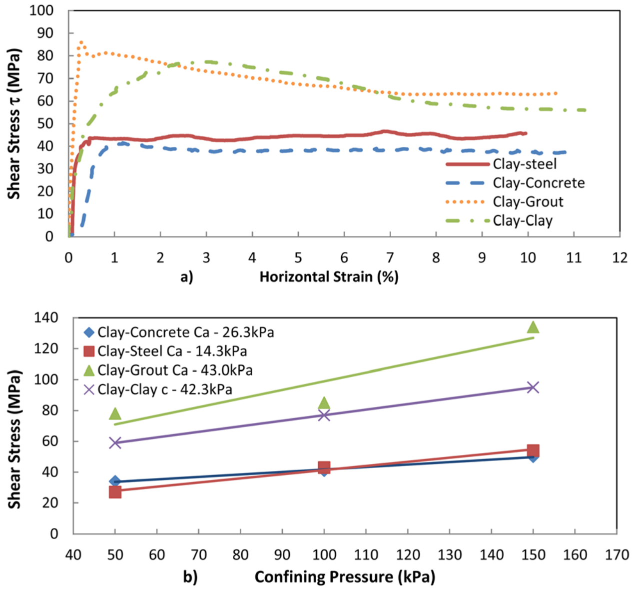

FIG. 5—*(a) Shear stress-strain at 100 kPa. (b) Failure envelopes under undrained conditions.*

J_ID: ACEM DOI: 10.1520/ACEM20120043 Date: 3-September-13 Stage: Page: 11 Total Pages: 18

PROOF COPY [ACEM20120043]

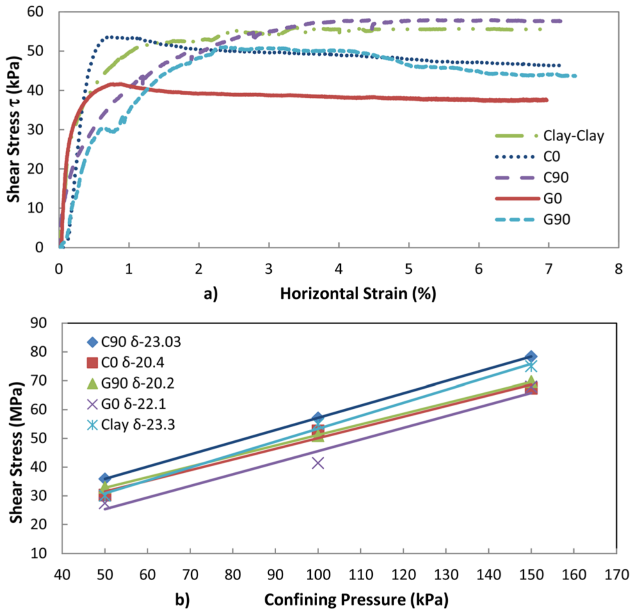

FIG. 6—*(a) Shear stress-strain curve at 100 kPa. (b) Failure envelopes for FRP under drained conditions.*

Fiber-reinforced Polymer Interface Shear Strength

In this section, the interface shear strength of clay and FRP materials (carbon and glass) oriented at 90° and at 0° along the primary fiber is investigated. The goal is to determine whether the greater waviness of the FRP surfaces (Fig. 2) contributes to higher shear strength values when sheared against clay and, if so, identify which FRP material and orientation provides optimal results.

Drained Conditions

The direct shear tests carried out with the FRP specimens were analogous to the tests conducted on their steel, concrete, and grout counterparts. Figure 6(*a*) shows the shear stress-strain curves for the four FRP coupons, along with the results for the clay. The displacement required in order to mobilize friction along the FRP interfaces was in the range of 0.3 % to 0.5 %, and residual strength conditions were reached by G0 and C0 interfaces at 1.4 %, whereas G90 and C90 showed strain hardening behavior, reaching a constant strength at approximately 3.5 % strain. The FRP specimens G0 and C0 also experienced a slight stress relaxation past the peak shear strength reached, whereas G90, C90, and pure clay maintained a constant residual strength at or near their peak shear strength.

Figure 6(*b*) presents the failure envelope results for each of the FRP interfaces and their respective drained effective interface friction angles δ. Table 3 summarizes the ratio of the interface friction angle to the soil's internal friction angle δ/Φ'. In all cases, the interface friction angle corresponds to a value between 0.86ϕ and 0.98ϕ, with the C90 specimen presenting the highest value and G0 the lowest, although the results for all FRP specimens fall within a narrow range of 12 % variation. When we compare these results to those obtained for steel and concrete, we see that FRP interfaces demonstrated reduced frictional resistance relative to concrete and grout, but a slightly greater friction angle (5 % to 19 %) than the steel interface.

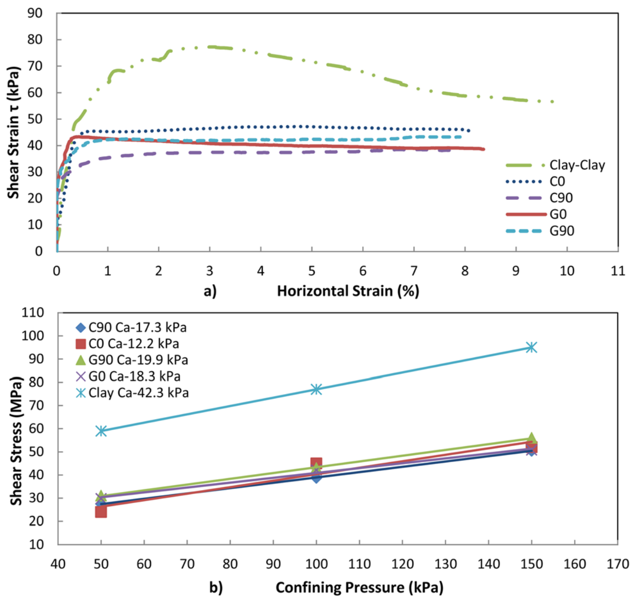

FIG. 7—*(a) Shear stress-strain at 100 kPa. (b) Failure envelopes for FRP under undrained conditions.*

Undrained Conditions

The results for undrained conditions for the FRP samples show the apparent cohesion values of each interface. Figure 7(*a*) presents the shear stress-strain curves for the FRP interfaces and clay at a confining pressure of 100 kPa. The results show that all four FRP interfaces presented very similar shearing behaviors under the fast loading rate. All the FRP specimens mobilized the frictional capacity at a very low strain of 0.1 % to 0.2 % and reached a maximum shear strength value at a strain of 1 % that remained virtually constant throughout the shearing. For a confining pressure of 100 kPa, the residual shear strength of the four FRP specimens presented a very narrow spread at 47 kPa for C0 and 40 KPa for C90 for the highest and lowest values, respectively. Relative to the shearing behavior of clay, all the FRP specimens showed significantly lower shear strength values at a confining pressure of 100 kPa.

Figure 7(*b*) shows the failure envelopes of each of the FRP interfaces, and Table 3 summarizes these results and compares the calculated apparent interface adhesion c_a to the measured soil cohesion c. The ratio c_a/c indicates that for FRP specimens, the interface adhesion was between 40 % and 47 % of that of the soil, and in particular, the carbon interface C0 had a significantly lower value at 28 % of that of the soil. When we compare these results to the previously presented values for steel and concrete, we see that FRP interfaces demonstrated reduced performance relative to concrete and grout but a similar or greater adhesion relative to the steel interface.

Discussion

Pile–Soil and Fiber-reinforced Polymer–Soil Interface Performance

The interface performance of both traditional pile materials and FRPs was evaluated and compared in order to assess the viability of FRP relative to current piling materials. The results have been analyzed with respect to the performance of each material in both drained and undrained conditions, and the compiled results of the testing program are summarized in Table 3.

The drained tests on the traditional piling materials indicated strong frictional shear resistance from the grout and concrete elements and moderate resistance from the steel interface. These results support the idea of the development of turbulent shearing mechanisms along the concrete and grout interfaces due to disturbance of the clay particles at the interface microstructure and the development of sliding or transitional shearing mechanisms along the steel interface. It is difficult to assess the influence of surface roughness, as both steel and concrete demonstrated similar surface roughness values at $R_t = 9.7$ and $R_t = 7.5$, respectively. The most likely influencing factor is the reduction of pore pressure at the concrete interface due to the absorption of pore water by the concrete. In addition, ion exchange between the concrete interstitial fluid and soil pore water can increase the soil salinity, in turn increasing its shear strength [13]. The grout shearing strength demonstrated the highest frictional capacity as a result of several possible factors: the development of a bonding region between the clay and grout during the curing period; water absorption by the grout as part of the hydration process of the cement, which in turn reduces pore pressures generated at the interfaces; and the development of surface irregularities at the shearing interface when the grout–soil bonding is broken apart upon shearing. Upon visual inspection of the sheared surface, it was evident that a bonding region roughly 1 mm thick between the soil and the grout had formed. This soil–grout bonding allows for the development of high shearing resistance and, as such, is the basis for the design of soil nails and micropiles.

The interface-to-soil friction angle ratios δ/ϕ deviated slightly from the common values typically used in practice, which advocates the use of $2/3\phi'$ as a reasonable value for the interface frictional angle δ [24]. The steel–clay interface values present reasonable correlation with the typically used data, whereas the concrete–clay and grout–clay interfaces had higher ratios. The concrete–clay interface exhibited turbulent shearing due to the absorption of water at the interface, which can have the net effect of increasing the friction angle values. At the grout interface, soil–grout bonding and the absorption of water by the grout mixture can have similar effects.

The FRP interface test results under drained conditions showed less interface resistance strength relative to concrete and grout while presenting an angle of friction up to 19 % greater than that seen with the steel interfaces. From these results it can be concluded that the surface waviness of the FRP materials probably affected the interface frictional capacity in clays, particularly relative to steel interfaces. Upon inspection of the sheared interfaces it was identified that, in some instances, the clay material was wedged in between the ridges formed by the FRP surface, and shearing of the clay occurred along the flat plane in between the ridges. This behavior was identified more often on the specimens sheared perpendicular to the fiber orientation (i.e., the 90° orientation). In other instances, the clay material showed evidence of sliding along the grooves of the ridges presented in the FRP fiber. This type of behavior would occur more frequently on the specimens sheared along the fiber orientation (i.e., the 0° orientation). In both cases, it is possible that the clay particles undergo shearing by particle sliding or turbulent shear failure, evidenced by the higher measured friction angle of FRP interfaces over steel. Based on these results, it is difficult to assess with certainty which material and which fiber orientation present the best results, as the differences are within 15 %. Pile load tests are needed in order to best establish the material performance under field conditions.

The performance under undrained conditions followed a trend similar to that of the drained conditions with respect to the higher adhesion values of grout and concrete. However, results for FRP and steel show that FRP interfaces presented an interface adhesion improvement between 20 % and 35 % greater for G90, G0, and C90, whereas C0 presented a lower interface adhesion that was 85 % that of steel. As discussed earlier, this could be attributed to the smoother surface of the steel interface relative to FRPs, and hence the associated shearing mechanisms involved for both cases (sliding versus turbulence). Similar to the drained results, the variation in the adhesion values for the top three FRP interfaces is within 15 %, making it difficult to determine which material or orientation provides better performance.

Considering both drained and undrained conditions, FRP materials present less shear strength resistance than concrete or grouted interfaces; however, their presented performance is better than or comparable to that of steel interfaces. The introduction of FRP piles in the FRP industry could lead to possible cost reductions due to the effect of economies of scale in the composite industry as demand increases. Through communication with the FRP manufacturer, it was found that at the time of publication, the price of the CFRP raw materials was double that of the GFRP fibers per unit area (R. Ortiz, personal communication, May 2012). Further work is needed regarding the cost benefit of carbon fibers versus glass fibers in terms of pile performance.

Effect of Epoxy Resin on Interface Behavior

During the experimental program, it was observed that the manufacturing process of casting the fiber composites in an epoxy matrix created a smooth, although topographically varied, FRP surface. To investigate the effects of the epoxy resin on the interface frictional behavior, an additional test using a dry (i.e., no epoxy encasement) C90 specimen was conducted with the purpose of evaluating whether or not the individual fibers interacted with the soil particles to influence the interface shear behavior.

The additional test was conducted by placing an appropriately cut portion of dry carbon fiber on top of the steel specimen used in previous interface tests. This steel plate was bolted to the top half of the shear box, ensuring that the C90 specimen was securely in place. A soil specimen was then placed in the top half of the shear box, and then a drained shearing test was conducted in the same manner as described above. Special care was taken to prevent any possible sliding of the FRP sample against the steel plate support by placing an extended portion of the material underneath the shear box, thus using the confining pressure for clamping action.

Figure 8 presents the shear stress-strain curves for dry-fiber C90, epoxy-encased C90, and soil at 100-kPa confining pressure under a drained shearing rate. The results from these tests indicate that although the material fabrics were free to interact with the soil particles, the behavior was significantly softer than that of the epoxy-cast C90 specimen. Upon visual inspection of the sheared surface, both the clay and the FRP surface presented minimal disturbance, suggesting a sliding type of

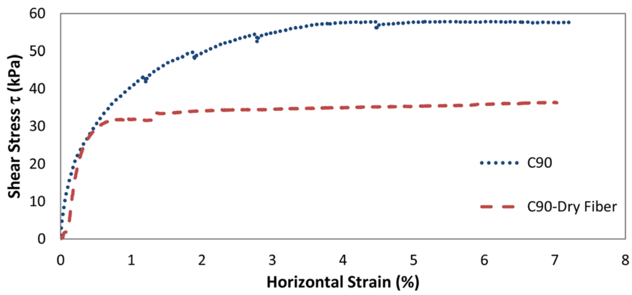

FIG. 8—*Comparison of dry fiber (no epoxy) and regular FRP performance under a confining pressure of 100 kPa (drained condition).*

shear failure across the interface. The interface friction angle of the C90 dry-fiber sample was calculated as $\delta = 19.3°$, which is 83 % of the friction angle calculated for the epoxy-cast C90 specimen. These results show that there is no merit in pursuing uncased fabric material interaction; in addition, it is impractical to use the material in this uncured state.

Conclusions

An experimental program was carried out with the goal of determining the interface shear strength properties of various typical pile materials and two different fiber-reinforced composite materials against soft clay. The test results were used to quantify the performance of each interface and evaluate the viability of FRP materials relative to typical piling materials. The experimental program used a direct shear box device intended to measure the interface friction angle and the apparent interface adhesion, and tests were carried out under drained and undrained conditions. The following points illustrate the main findings of this paper:

- In both drained and undrained conditions, the concrete and grout piling materials outperformed the FRP interfaces, but the FRP specimens matched or performed better than the steel interface under both loading rates.
- Grout presented the highest shear strength parameters, a result that was expected, as grout forms a strong grout–soil bonding region during the curing process.
- The concrete interface presented a high interface frictional coefficient with a δ/ϕ ratio of 1.12. This result is higher than the typically used ratio of 0.5 to 0.7 and could be caused by the absorption of water by the concrete, which would decrease the pore pressure at the interface.
- The steel interface displayed a lower capacity than concrete in both drained and undrained conditions, indicating a sliding type of shear failure at the interface, in contrast to concrete, which presented evidence of turbulent or transitional shear failure.
- The FRP materials presented between 105 % and 119 % of the interface friction angle of steel and between 77 % and 88 % that of concrete. In addition, FRP interface adhesion was observed between 86 % and 135 % of the interface adhesion of steel and between 65 % and 75 % of the interface adhesion of concrete.
- The results indicate that the best performing FRP interface was CFRP oriented at 90° with respect to the primary fiber (C90) in drained conditions and GFRP oriented at 90° with respect to the primary fiber (G90) under undrained conditions. However, the capacity increase, particularly relative to G90 and C0, was not significant enough for a superior material (carbon or glass) or fiber orientation along the shearing direction (0° or 90°) to be conclusively determined. Specimen C0 was the only exception under undrained conditions, with approximately 35 % less interface adhesion than the other three FRP interfaces.
- FRP surface topology and the waviness pattern dictated by the fiber weaving and orientation during shearing were found to have a possibly significant influence on the shearing strength.
- Investigation into the effect of the epoxy surface finish was carried out and indicated lower frictional performance relative to the epoxy-cast specimen.
- In order to account for other parameters such as FRP moduli and installation effects due to pile driving, full-scale pile load tests are needed to validate the results found in this research program.

The results presented in this study show that FRP piles constructed using carbon or glass fibers can perform at the same level as or better than traditional steel piling under both drained and undrained conditions in clays. This finding is coupled with major advantages of FRPs such as their corrosion resistance and longer service life, areas in which steel piling presents weaknesses. FRP interfaces were found to possess 105 % to 119 % of the capacity of steel against clays under frictional behavior and between 86 % and 135 % of interface adhesion. Further work should focus on the effect of a roughened epoxy surface (without compromising the fiber integrity) to accurately quantify the effects of the surface roughness of FRP shearing against clays and on pile load tests to simulate interface behavior under field circumstances.

Acknowledgments

This research was financially supported by the Natural Science and Engineering Research Council of Canada (NSERC). The writers are grateful to their industrial partner FYFE Co. LLC; however, the views expressed herein are those of the writers and not necessarily those of their partner.

References

[1] Lemos, L. J. L. and Vaughan, P. R., "Clay-Interface Shear Resistance," *Geotechnique*, Vol. 50(1), 2000, pp. 55–64.

[2] Rouaiguia, A., "Residual Shear Strength of Clay-Structure Interfaces," *Int. J. Civil and Enviro. Eng.*, Vol. 10(3), 2010, pp. 6–18.

[3] Iskander, M. G. and Hassan, M., "State of the Practice Review in Composite Piling," *J. Compos. Constr.*, Vol. 2(3), 1998, pp. 116–120.

[4] Frost, J. D. and Han, J., "Behaviour of Interfaces between Fiber-reinforced Polymers and Sands," *J. Geotech. Geoennviron. Eng.*, Vol. 125(8), 1999, pp. 633–640.

[5] Pando, A. M., Flitz, M. G., Dove, J. E., and Hoppe, E. J., "Interface Shear Tests on FRP Composite Piles," *International Deep Foundations Congress*, Orlando, FL, Feb. 14–16, 2002, ASCE, Reston, VA, pp. 1486–1500.

[6] Chu, L. M. and Yin, J. H., "Study on Soil–Cement Grout Interface Shear Strength of Soil Nailing," *Geomech. Geoeng.*, Vol. 1(4), 2006, pp. 259–273.

[7] Skempton, A. W., "Long Term Stability of Clay Slopes," *Geotechnique*, Vol. 14(2), 1964, pp. 77–102.

[8] Lupini, J. F., Skinner, A. E., and Vaughan, P. R., "Drained Residual Strength of Cohesive Soils," *Geotechnique*, Vol. 31(2), 1981, pp. 181–213.

[9] Stark, T. and Eid, H. T., "Drained Residual Strength of Cohesive Soils," *J. Geotech. Engrg.*, Vol. 120(5), 1994, pp. 856–871.

[10] Goh, A. T. C. and Donald, I. B., "Investigation of Soil-Concrete Interface by Simple Shear Apparatus," *Fourth Australia-New Zealand Conference on Geomechanics*, Perth, Australia, May 14–18, 1984.

AQ1

[11] Johnston, I. W., Lam, T. S. K., and Williams, A. F., "Constant Normal Stiffness Direct Shear Testing for Socketed Pile Design in Weak Rock," *Geotechnique*, Vol. 37(1), 1987, pp. 83–89.

[12] Ovando-Shelley, E., "Direct Shear Tests on Mexico City Clay With Reference to Friction Pile Behavior," *Geotech. Geologic. Eng.*, Vol. 13, 1995, pp. 1–16.

[13] Taha, A. M., 2010, "Interface Shear Behaviour of Sensitive Marine Clay—Leda Clay," M.S. thesis, University of Ottawa, Ottawa, ON, Canada.

[14] ASTM D4318-10: Standard Test Methods for Liquid Limit, Plastic Limit, and Plasticity Index of Soils, *Annual Book of ASTM Standards*, ASTM International, West Conshohocken, PA, 2010.

[15] ASTM D422-63: Standard Test Method for Particle-Size Analysis of Soils, *Annual Book of ASTM Standards*, ASTM International, West Conshohocken, PA, 2007.

[16] ASTM D2487-11: Standard Practice for Classification of Soils for Engineering Purposes (Unified Soil Classification System), *Annual Book of ASTM Standards*, ASTM International, West Conshohocken, PA, 2011.

[17] ASTM D2573-08: Standard Test Method for Field Vane Shear Test in Cohesive Soil, *Annual Book of ASTM Standards*, ASTM International, West Conshohocken, PA, 2011.

[18] ASTM D2435/2435M-11: Standard Test Methods for One-dimensional Consolidation Properties of Soils Using Incremental Loading, *Annual Book of ASTM Standards*, ASTM International, West Conshohocken, PA, 2011.

[19] ASTM D3080/D3080M-11: Standard Test Method for Direct Shear Test of Soils Under Consolidated Drained Conditions, *Annual Book of ASTM Standards*, ASTM International, West Conshohocken, PA, 2012.

[20] Silvestri, V., Karam, G., Tonthat, A., and St-Amour, Y., "Direct and Simple Shear Testing of Two Canadian Sensitive Clays," *Geotech. Test. J.*, Vol. 12(1), 1989, pp. 11–21.

[21] Potyondy, J. G., "Skin Friction between Various Soils and Interface and Construction Materials," *Geotechnique*, Vol. 11(4), 1961, pp. 3–18.

[22] Yoshimi, Y. and Kishida, T., "A Ring Torsion Apparatus for Evaluating Friction between Soil and Metal Surfaces," *Geotech. Test. J.*, Vol. 4(4), 1981, pp. 145–152.

[23] O'Rourke, T. D., Drusche, l. S. J., and Netravali, A. N., "Shear Strength Characteristics of Sand-Polymer Interfaces," *J. Geotech. Engrg.*, Vol. 116(3), 1990, pp. 451–469.

[24] Canadian Geotechnical Society, *Canadian Geotechnical Engineering Manual*, 4th ed., BiTech Publishers Ltd., Richmond, BC, Canada, 2007.

[25] Kishida, H. l. and Uesegui, H., "Tests of the Interface between Sand and Steel in Simple Shear Apparatus," *Geotechnique*, Vol. 37(1), 1987, pp. 45–52.

[26] ASTM D5321-08: Standard Test Method for Determining the Coefficient of Soil and Geosynthetic or Geosynthetic and Geosynthetic Friction by the Direct Shear Method, *Annual Book of ASTM Standards*, ASTM International, West Conshohocken, PA, 2008.